

The effect of defect layer on transmissivity and light field distribution in general function photonic crystals

Xiang-Yao Wu^a, Si-Qi Zhang^a, Bo-Jun Zhang^a, Xiao-Jing Liu^a,
Jing Wang^a, Hong Li^a, Nuo Ba^a and Xin-Guo Yin^b

^a*Institute of Physics, Jilin Normal University, Siping 136000, China*

^b*Institute of Physics, Xuzhou Normal University, Xuzhou 221000, China*

We have theoretically investigated a general function photonic crystals (GFPCs) with defect layer, and choose the line refractive index function for two mediums A and B , and analyze the effect of defect layer's position, refractive indexes and period numbers on the transmission intensity and the electric field distribution. We obtain some new characters that are different from the conventional PCs, which should be helpful in the design of photonic crystals.

PACS: 42.70.Qs, 78.20.Ci, 41.20.Jb

Keywords: General photonic crystals; Defect model; Transmissivity; Light field distribution;

PACS numbers:

1. Introduction

Photonic crystals (PC) are a new kind of mater which facilitate the control of the light [1]. PC exhibit Photonic Band Gaps (PBG) that forbids the radiation propagation in a specific range of frequencies [2-6]. A PBG forbids the radiation propagation in a specific range of frequencies. The existence of PBGs will lead to many interesting phenomena, e.g., modification of spontaneous emission [7-9] and photon localization [10]. Thus numerous applications of photonic crystals have been proposed in improving the performance of optoelectronic and microwave devices such as high-efficiency semiconductor lasers, light emitting diodes, wave guides, optical filters, high-Q resonators, antennas, frequency-selective surfaces, optical limiters and amplifiers [11-18]. In the past years has been developed an intensive effort to study micro-fabricate PBG materials in one, two or three dimensions [19-21]. In Refs. [22-25], we have proposed a general function photonic crystals (GFPCs), which refractive index is an arbitrary function of space position. Unlike conventional photonic crystals (PCs), which structure grow from two materials, A and B , with different dielectric constants ε_A and ε_B , and have obtained some results different from the conventional photonic crystals. In the paper, We have studied the general function photonic crystals (GFPCs) with defect layer, and choose the line refractive index function for two mediums A and B . We obtain some results: (1) When the position of defect layer move behind in the GFPCs, or the refractive indexes of defect layer increase, the transmission intensity maximum of defect model decreases. (2) When the period number of GFPCs increase, the transmission intensity of defect model increase, and the defect model's width of half height become narrow. (3) Both the defect layer and its position have the effects on the electric field. (4) In the structure $(BA)^N D(BA)^N$, when the period number N increase, the relative intensity of electric field increase. (5) When the refractive indexes of defect layer (n_d) increase, the relative intensity of electric field was enhanced.

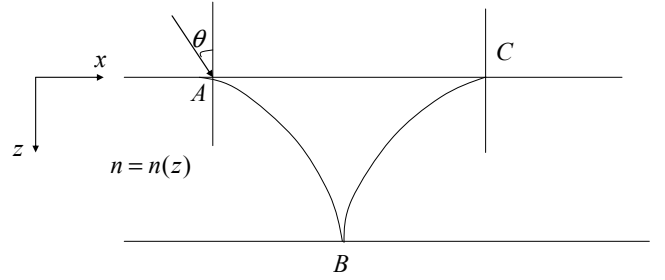


FIG. 1: The motion path of light in the medium of refractive index $n(z)$.

2. The light motion equation in general function photonic crystals

For the general function photonic crystals, the medium refractive index is a periodic function of the space position, which can be written as $n(z)$, $n(x, z)$ and $n(x, y, z)$ corresponding to one-dimensional, two-dimensional and three-dimensional function photonic crystals. In the following, we shall deduce the light motion equations of the one-dimensional general function photonic crystals, i.e., the refractive index function is $n = n(z)$, meanwhile motion path is on xz plane. The incident light wave strikes plane interface point A , the curves AB and BC are the path of incident and reflected light respectively, and they are shown in FIG. 1.

The light motion equation can be obtained by Fermat principle, it is

$$\delta \int_A^B n(z) ds = 0. \quad (1)$$

In the two-dimensional transmission space, the line element ds is

$$ds = \sqrt{(dx)^2 + (dz)^2} = \sqrt{1 + \dot{z}^2} dx, \quad (2)$$

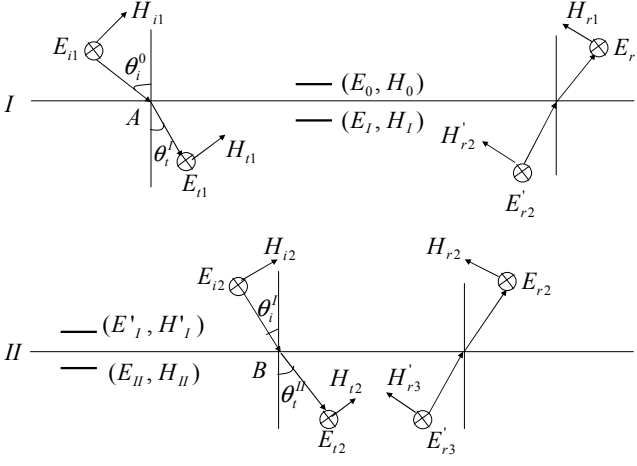


FIG. 2: The light transmission and electric magnetic field distribution figure in FIG.1 medium.

where $\dot{z} = \frac{dz}{dx}$, then Eq. (1) becomes

$$\delta \int_A^B n(z) \sqrt{1 + (\dot{z})^2} dx = 0. \quad (3)$$

The Eq. (3) change into

$$\int_A^B \left(\frac{\partial(n(z)\sqrt{1+\dot{z}^2})}{\partial z} \delta z + \frac{\partial(n(z)\sqrt{1+\dot{z}^2})}{\partial \dot{z}} \delta \dot{z} \right) dx = 0, \quad (4)$$

At the two end points A and B, their variation is zero, i.e., $\delta z(A) = \delta z(B) = 0$. For arbitrary variation δz , the Eq. (4) becomes

$$\begin{aligned} & \frac{dn(z)}{dz} \sqrt{1 + \dot{z}^2} - \frac{dn(z)}{dz} \dot{z}^2 (1 + \dot{z}^2)^{-\frac{1}{2}} \\ & - n(z) \frac{\ddot{z} \sqrt{1 + \dot{z}^2} - \dot{z}^2 \ddot{z} (1 + \dot{z}^2)^{-\frac{1}{2}}}{1 + \dot{z}^2} = 0, \end{aligned} \quad (5)$$

simplify Eq. (5), we have

$$\frac{dn(z)}{n(z)} = \frac{\dot{z} d\dot{z}}{1 + \dot{z}^2}. \quad (6)$$

The Eq. (6) is light motion equation in one-dimensional function photonic crystals.

3. The transfer matrix of one-dimensional general function photonic crystals

In this section, we should calculate the transfer matrix of one-dimensional general function photonic crystals. In fact, there is the reflection and refraction of light at a plane surface of two media with different dielectric properties. The dynamic properties of the electric field and magnetic field are contained in the boundary conditions: normal components of D and B are continuous; tangential components of E and H are continuous. We consider the electric field perpendicular to the plane of incidence,

and the coordinate system and symbols as shown in FIG. 2.

On the two sides of interface I, the tangential components of electric field E and magnetic field H are continuous, there are

$$\begin{cases} E_0 = E_I = E_{t1} + E'_{r2} \\ H_0 = H_I = H_{t1} \cos \theta_t^I - H'_{r2} \cos \theta_t^I. \end{cases} \quad (7)$$

On the two sides of interface II, the tangential components of electric field E and magnetic field H are continuous, and give

$$\begin{cases} E_{II} = E'_I = E_{i2} + E_{r2} \\ H_{II} = H'_I = H_{i2} \cos \theta_i^I - H_{r2} \cos \theta_i^I, \end{cases} \quad (8)$$

the electric field E_{t1} is

$$E_{t1} = E_{t10} e^{i(k_x x_A + k_z z)}|_{z=0} = E_{t10} e^{i \frac{\omega}{c} n(0) \sin \theta_t^I x_A}, \quad (9)$$

and the electric field E_{i2} is

$$\begin{aligned} E_{i2} &= E_{t10} e^{i(k'_x x_B + k'_z z)}|_{z=b} \\ &= E_{t10} e^{i \frac{\omega}{c} n(b) (\sin \theta_i^I x_B + \cos \theta_i^I b)}. \end{aligned} \quad (10)$$

Where x_A and x_B are x component coordinates corresponding to point A and point B. We should give the relation between E_{i2} and E_{t1} . By integrating the two sides of Eq. (6), we can obtain the coordinate component x_B of point B

$$\int_{n(0)}^{n(z)} \frac{dn(z)}{n(z)} = \int_{k_0}^{k_z} \frac{\dot{z} d\dot{z}}{1 + \dot{z}^2}, \quad (11)$$

to get

$$k_z^2 = (1 + k_0^2) \left(\frac{n(z)}{n(0)} \right)^2 - 1, \quad (12)$$

and

$$dx = \frac{dz}{\sqrt{(1 + k_0^2) \left(\frac{n(z)}{n(0)} \right)^2 - 1}}. \quad (13)$$

where $k_0 = \cot \theta_t^I$ and $k_z = \frac{dz}{dx}$. From Eq. (12), there is $n(z) > n(0) \sin \theta_t^I$. and the coordinate x_B is

$$x_B = x_A + \int_0^b \frac{dz}{\sqrt{(1 + k_0^2) \left(\frac{n(z)}{n(0)} \right)^2 - 1}}, \quad (14)$$

where b is the medium thickness of FIG. 1 and FIG. 2. By substituting Eqs. (9) and (14) into (10), and using the equality

$$n(0) \sin \theta_t^I = n(b) \sin \theta_i^I, \quad (15)$$

we have

$$E_{i2} = E_{t1} e^{i \delta b}, \quad (16)$$

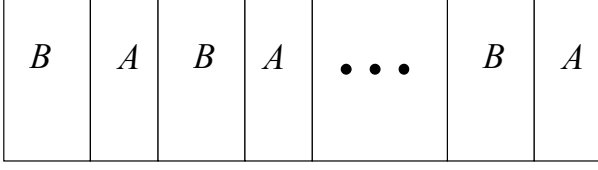


FIG. 3: The structure $(BA)^N$ of the general function photonic crystals.

where

$$\delta_b = \frac{\omega}{c} n_b(b) (\cos \theta_i^I b + \sin \theta_i^I \int_0^b \frac{dz}{\sqrt{\frac{n_b^2(z)}{n_0^2 \sin^2 \theta_i^0} - 1}}), \quad (17)$$

and similarly

$$E'_{r2} = E_{r2} e^{i\delta_b}. \quad (18)$$

Substituting Eqs. (16) and (18) into (7) and (8), and using $H = \sqrt{\frac{\varepsilon_0}{\mu_0}} n E$, we obtain

$$\begin{pmatrix} E_I \\ H_I \end{pmatrix} = M_B \begin{pmatrix} E_{II} \\ H_{II} \end{pmatrix}, \quad (19)$$

where

$$M_B = \begin{pmatrix} \cos \delta_b & -\frac{i \sin \delta_b}{\sqrt{\frac{\varepsilon_0}{\mu_0}} n_b(b) \cos \theta_i^I} \\ -in_b(0) \sqrt{\frac{\varepsilon_0}{\mu_0}} \cos \theta_i^I \sin \delta_b & \frac{n_b(0) \cos \theta_i^I \cos \delta_b}{n_b(b) \cos \theta_i^I} \end{pmatrix} \quad (20)$$

The Eq. (20) is the transfer matrix M in the medium of FIG. 1 and FIG. 2. By refraction law, we can obtain

$$\sin \theta_t^I = \frac{n_0}{n(0)} \sin \theta_i^0, \cos \theta_t^I = \sqrt{1 - \frac{n_0^2}{n^2(0)} \sin^2 \theta_i^0}, \quad (21)$$

where n_0 is air refractive index, and $n(0) = n(z)|_{z=0}$. Using Eqs. (15) and (21), we can calculate $\cos \theta_i^I$.

4. The transmissivity and light field distribution of one-dimensional general function photonic crystals

In section 3, we obtain the M matrix of the half period. We know that the conventional photonic crystals is constituted by two different refractive index medium, and the refractive indexes are not continuous on the interface of the two mediums. We could devise the one-dimensional general function photonic crystals structure as follows: in the first half period, the refractive index distributing function of medium B is $n_b(z)$. and in the second half period, the refractive index distributing function of medium A is $n_a(z)$, corresponding thicknesses are b and a , respectively. Their refractive indexes satisfy condition $n_b(b) \neq n_a(0)$, their structure are shown in FIG. 3, and FIG. 4. The Eq. (20) is the half period transfer

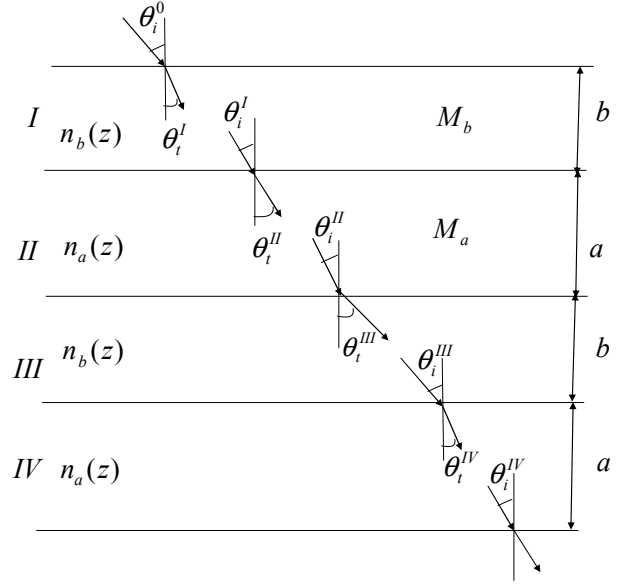


FIG. 4: The two periods transmission figure of light in general function photonic crystals.

matrix of medium B . Obviously, the half period transfer matrix of medium A is

$$M_A = \begin{pmatrix} \cos \delta_a & -\frac{i \sin \delta_a}{\sqrt{\frac{\varepsilon_0}{\mu_0}} n_a(a) \cos \theta_i^{II}} \\ -in_a(0) \sqrt{\frac{\varepsilon_0}{\mu_0}} \cos \theta_i^{II} \sin \delta_a & \frac{n_a(0) \cos \theta_i^{II} \cos \delta_a}{n_a(a) \cos \theta_i^{II}} \end{pmatrix} \quad (22)$$

where

$$\delta_a = \frac{\omega}{c} n_a(a) [\cos \theta_i^{II} \cdot a + \sin \theta_i^{II} \int_0^a \frac{dz}{\sqrt{\frac{n_a^2(z)}{n_0^2 \sin^2 \theta_i^0} - 1}}], \quad (23)$$

$$\cos \theta_t^{II} = \sqrt{1 - \frac{n_0^2}{n_a^2(0)} \sin^2 \theta_i^0}, \quad (24)$$

and

$$\sin \theta_i^{II} = \frac{n_0}{n_a(a)} \sin \theta_i^0, \quad (25)$$

$$\cos \theta_i^{II} = \sqrt{1 - \frac{n_0^2}{n_a^2(a)} \sin^2 \theta_i^0}. \quad (26)$$

In one period, the transfer matrix M is

$$\begin{aligned} M &= M_B \cdot M_A \\ &= \begin{pmatrix} \cos \delta_b & \frac{-i \sin \delta_b}{\sqrt{\frac{\varepsilon_0}{\mu_0}} n_b(b) \cos \theta_i^I} \\ -in_b(0) \sqrt{\frac{\varepsilon_0}{\mu_0}} \cos \theta_i^I \sin \delta_b & \frac{n_b(0) \cos \theta_i^I \cos \delta_b}{n_b(b) \cos \theta_i^I} \end{pmatrix} \\ &\quad \begin{pmatrix} \cos \delta_a & \frac{-i \sin \delta_a}{\sqrt{\frac{\varepsilon_0}{\mu_0}} n_a(a) \cos \theta_i^{II}} \\ -in_a(0) \sqrt{\frac{\varepsilon_0}{\mu_0}} \cos \theta_i^{II} \sin \delta_a & \frac{n_a(0) \cos \theta_i^{II} \cos \delta_a}{n_a(a) \cos \theta_i^{II}} \end{pmatrix} \end{aligned} \quad (27)$$

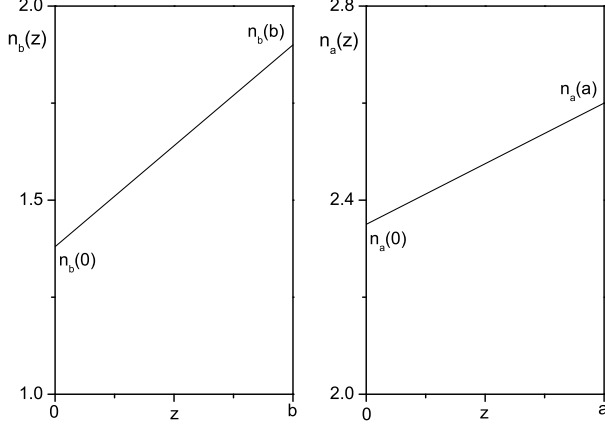


FIG. 5: The refractive index of the general functions in a period.

The defect layer's refractive index is constant n_d , its transfer matrix M_d is

$$M_d = \begin{pmatrix} \cos \delta_d & -\frac{i}{\eta_d} \sin \delta_d \\ -i\eta_d \sin \delta_d & \cos \delta_d \end{pmatrix}, \quad (28)$$

where $\eta_d = \sqrt{\frac{\varepsilon_0}{\mu_0}} n_d$, $\delta_d = \frac{\omega}{c} n_d d$.

The form of the GFPCs transfer matrix M is more complex than the conventional PCs. The angle θ_t^I , θ_i^I , θ_t^{II} and θ_i^{II} are shown in Fig. 4. The characteristic equation of GFPCs is

$$\begin{aligned} \begin{pmatrix} E_1 \\ H_1 \end{pmatrix} &= M_1 M_2 \cdots M_d \cdots M_N \begin{pmatrix} E_{N+1} \\ H_{N+1} \end{pmatrix} \\ &= M_b M_a M_b M_a \cdots M_d \cdots M_b M_a \begin{pmatrix} E_{N+1} \\ H_{N+1} \end{pmatrix} \\ &= M \begin{pmatrix} E_{N+1} \\ H_{N+1} \end{pmatrix} = \begin{pmatrix} A & B \\ C & D \end{pmatrix} \begin{pmatrix} E_{N+1} \\ H_{N+1} \end{pmatrix}. \end{aligned} \quad (29)$$

Where N is the period number. With the transfer matrix M (Eq. (28)), we can obtain the transmission and reflection coefficient t and r , and the transmissivity and reflectivity T and R , they are

$$t = \frac{E_{tN+1}}{E_{i1}} = \frac{2\eta_0}{A\eta_0 + B\eta_0\eta_{N+1} + C + D\eta_{N+1}}, \quad (30)$$

$$r = \frac{E_{r1}}{E_{i1}} = \frac{A\eta_0 + B\eta_0\eta_{N+1} - C - D\eta_0}{A\eta_0 + B\eta_0\eta_{N+1} + C + D\eta_0}, \quad (31)$$

and

$$T = t \cdot t^*, \quad (32)$$

$$R = r \cdot r^*. \quad (33)$$

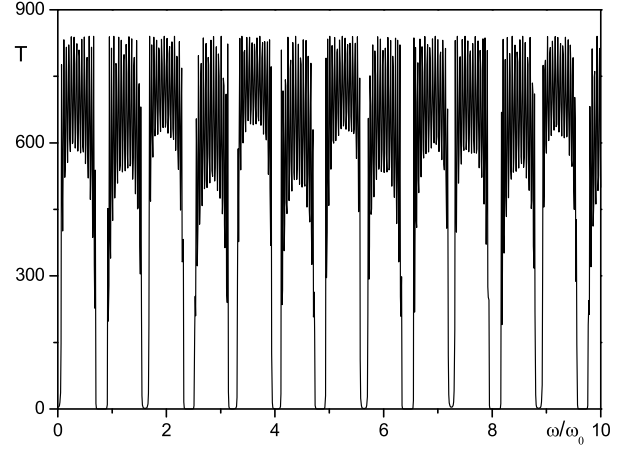


FIG. 6: The relation between transmissivity and frequency corresponding to the general function photonic crystals.

Where $\eta_0 = \eta_{N+1} = \sqrt{\frac{\varepsilon_0}{\mu_0}}$. In the following, we give the electric field distribution of light in the one-dimensional GFPCs. The propagation figure of light in one-dimensional GFPCs is shown in FIG. 9. From Eq. (28), we have

$$\begin{aligned} \begin{pmatrix} E_1 \\ H_1 \end{pmatrix} &= M_1(d_1) M_2(d_2) \cdots M_d(d) \cdots M_{N-1}(d_{N-1}) \\ &M_N(\Delta z_N) \begin{pmatrix} E_N(d_1 + d_2 \cdots + d_{N-1} + \Delta z_N) \\ H_N(d_1 + d_2 \cdots + d_{N-1} + \Delta z_N) \end{pmatrix} \end{aligned} \quad (34)$$

where d_1 and d_2 are the thickness of first and second period, respectively, Δz_N is the propagation distance of light in the N -th period, E_1 and H_1 are the intensity of incident electric field and magnetic field, and $E_N(d_1 + d_2 \cdots + d_{N-1} + \Delta z_N)$ and $H_N(d_1 + d_2 \cdots + d_{N-1} + \Delta z_N)$ are the intensity of the N -th period electric field and magnetic field. The Eq. (34) can be written as

$$\begin{aligned} \begin{pmatrix} E_N(d_1 + d_2 \cdots + d_{N-1} + \Delta z_N) \\ H_N(d_1 + d_2 \cdots + d_{N-1} + \Delta z_N) \end{pmatrix} &= M_N^{-1}(\Delta z_N) \\ M_{N-1}^{-1}(d_{N-1}) \cdots M_2^{-1}(d_2) M_1^{-1}(d_1) \begin{pmatrix} E_1 \\ H_1 \end{pmatrix} \\ &= \begin{pmatrix} A(\Delta z_N) & B(\Delta z_N) \\ C(\Delta z_N) & D(\Delta z_N) \end{pmatrix} \begin{pmatrix} E_1 \\ H_1 \end{pmatrix}, \end{aligned} \quad (35)$$

the electric field E_1 and magnetic field H_1 can be written as

$$E_1 = E_{i1} + E_{r1} = (1 + r)E_{i1}, \quad (36)$$

$$\begin{aligned} H_1 &= H_{i1} \cos \theta_i^0 - H_{r1} \cos \theta_i^0 \\ &= \sqrt{\frac{\varepsilon_0}{\mu_0}} \cos \theta_i^0 (1 - r) E_{i1}. \end{aligned} \quad (37)$$

From Eqs. (34)-(36), we can obtain the ratio of the electric field $E_N(d_1 + d_2 \cdots + d_{N-1} + \Delta z_N)$ within the GFPCs to the incident electric field E_{i1} , it is

$$\begin{aligned} & \left| \frac{E_N(d_1 + d_2 \cdots + d_{N-1} + \Delta z_N)}{E_{i1}} \right|^2 \\ &= |A(\Delta z_N)(1+r) + B(\Delta z_N) \sqrt{\frac{\epsilon_0}{\mu_0}} \cos \theta_i^0 (1-r)|^2 \end{aligned} \quad (38)$$

5. Numerical result

In this section, we report our numerical results of transmissivity and light field distribution. We consider refractive indexes of the linearity functions in a period, it is

$$n_b(z) = n_b(0) + \frac{n_b(b) - n_b(0)}{b} z, \quad 0 \leq z \leq b, \quad (39)$$

$$n_a(z) = n_a(0) + \frac{n_a(a) - n_a(0)}{a} z, \quad 0 \leq z \leq a, \quad (40)$$

Eqs. (38) and (39) are the line refractive indexes distribution functions of two half period mediums B and A . When the endpoint values $n_b(0)$, $n_b(b)$, $n_a(0)$ and $n_a(a)$ are all given, the line refractive index functions $n_b(z)$ and $n_a(z)$ are ascertained. The main parameters are: the half period thickness b and a , the starting point refractive indexes $n_b(0)$ and $n_a(0)$, and end point refractive indexes $n_b(b)$ and $n_a(a)$, the optical thickness of the two mediums are equal, i.e., $n_b(0)b = n_a(0)a$, the incident angle $\theta_i^0 = 0$, the center frequency $\omega_0 = 1.215 \times 10^{15} \text{ Hz}$, the center wave length $\lambda_0 = \frac{2\pi c}{\omega_0}$, the thickness $b = 280 \text{ nm}$, $a = 165 \text{ nm}$ and the period number $N = 16$. we take $n_b(0) = 1.38$, $n_b(b) = 1.9$ for the medium B , and $n_a(0) = 2.35$, $n_a(a) = 2.6$ for the medium A , which are the up line function of refractive indexes, it is shown in FIG.5. By the refractive indexes function, we can calculate the transmissivity, we obtain the transmissivity distribution in FIG.6.

In FIG.7, we take $n_b(0) = n_b(b) = 1.38$, $n_a(0) = n_a(a) = 2.35$, i.e., the transmissivity of conventional photonic crystals. Compare FIG.6 with FIG.7, it can be found the results: (1) when the line function of refractive indexes is up, i.e., the GFPCs, the transmissivity can be far larger than 1 (T maximum is about 850), while the maximum of transmissivity in conventional photonic crystals is 1; (2) The number of band gaps in GFPCs are more than the conventional PCs.

In FIGs.8-10, we main discuss the relation between transmissivity and wave length corresponding to the GFPCs with defect layer, there is $n_d d = \frac{\lambda_0}{4}$. Base on the structure of GFPCs $(BA)^{16}$, we inset the defect layer at different position, which are shown in FIG.8(a-c). The structures are: (a) $(BA)^8 D (BA)^8$, (b) $(BA)^{10} D (BA)^6$, (c) $(BA)^{12} D (BA)^4$, where $n_d = 2$. We can see that when the position of defect layer is changed, the defect model become small. In FIG.9, we compare the transmissivity with different structure as $(BA)^N D (BA)^N$. In FIG.9(a-c), the half period number are: $N = 6$, $N = 7$ and

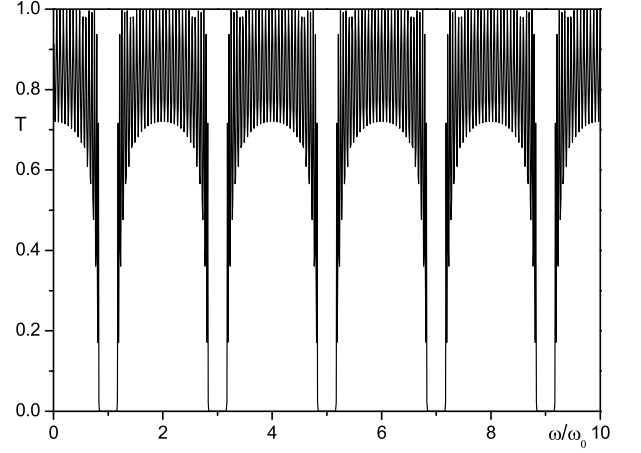


FIG. 7: The relation between transmissivity and frequency corresponding to the conventional photonic crystals.

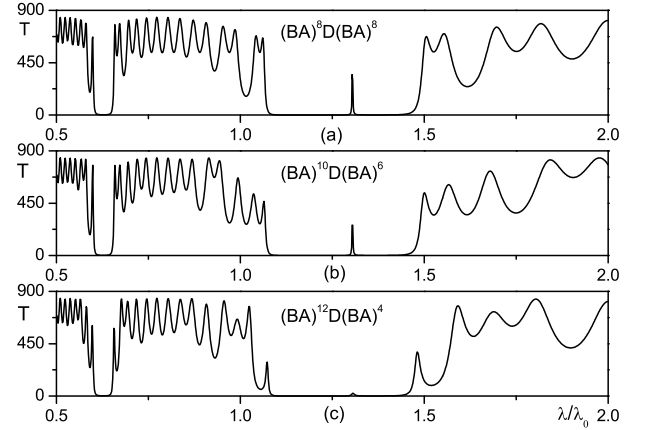


FIG. 8: Comparing the transmissivity of the GFPCs with different position of defect layer.

$N = 8$, where $n_d = 2$. We can obtain the results: As the number of half period N increase, for example, $N = 6$, the maximum of defect model achieve 110 (FIG.9(a)). When $N = 7$, the intensity of defect model is about 250 (FIG.9(b)). When N increases up to 8 (FIG.9(c)), the maximum of defect model nearly 400, i.e., as the half period number N increase, the maximum of defect model increase, the defect model's width of half height become narrow and the transmissivity of the GFPCs also increase.

FIG.10 shows the transmissivity of the GFPCs $((BA)^8 D (BA)^8)$ with different refractive indexes of defect layer. From FIG.10(a-c), n_d are taken as: 1.5, 2 and 5, respectively. Here, we notice that as the refractive indexes of defect layer increase, the intensity of defect

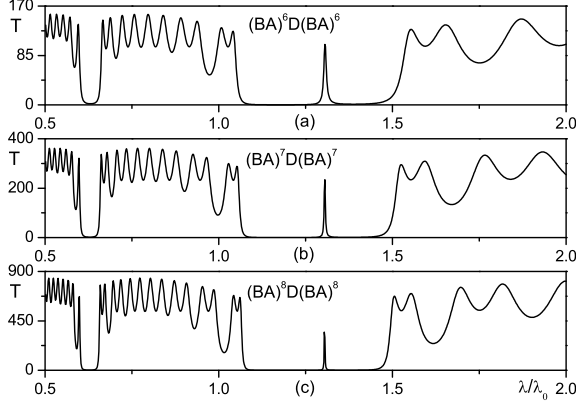


FIG. 9: Comparing the transmissivity of the GFPCs $((BA)^N D(BA)^N)$ with different half period numbers (a) $N=6$ (b) $N=7$ (c) $N=8$.

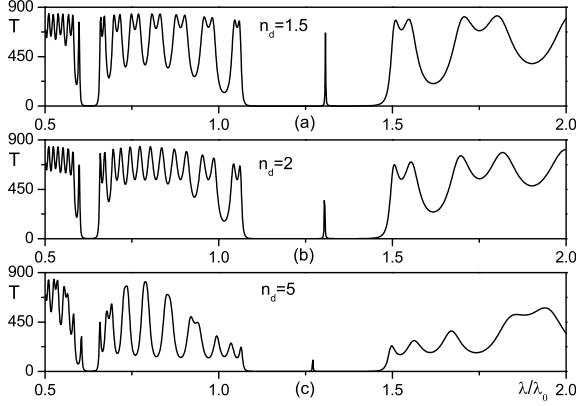


FIG. 10: Comparing the transmissivity of the GFPCs $((BA)^8 D(BA)^8)$ with different refractive indexes of defect layer.

model decrease, and the position of defect model become blue shift.

FIGS.11-14 are the distribution of electric field. The transverse axis z is propagation distance, and the longitudinal axis is the ratio of field intensity E and incidence field intensity E_{i1} square, i.e., $|E/E_{i1}|^2$.

FIG.11 is the distribution of electric field in conventional PCs. The structure of FIG.11(a-b) are $(BA)^{16}$ and $(BA)^8 D(BA)^8$. The main parameters are the same as FIG.7, and the $n_d = 2$, $n_{d1} = \frac{\lambda_0}{4}$. It can be found that the electric field was enhanced obviously when inserted the defect layer.

In the following, the main parameters are the same as FIG.6. In FIG.12, we study the effect of different structure of GFPCs on the distribution of light field. For FIG.12(a), the structure is $(BA)^{16}$, FIG.12(b)

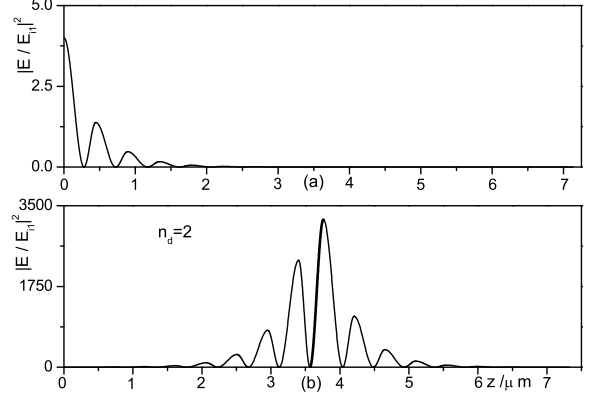


FIG. 11: The light distribution in the conventional PCs. (a) without the defect layer $((BA)^{16})$, (b) with the defect layer $((BA)^8 D(BA)^8)$. The bold line is the field distribution of defect layer.

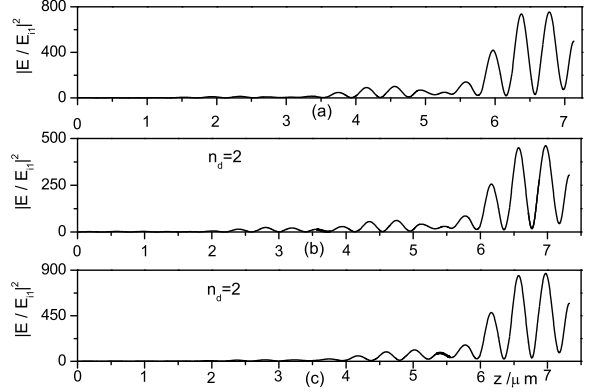


FIG. 12: The light distribution in the GFPCs. The structures are: (a) $(BA)^{16}$, (b) $(BA)^8 D(BA)^8$, (c) $(BA)^{12} D(BA)^4$. The bold line is the field distribution of defect layer.

and FIG.12(c), the structure are $(BA)^8 D(BA)^8$ and $(BA)^{12} D(BA)^4$, where $n_d = 2$, $n_{d1} = \frac{\lambda_0}{4}$. Comparing FIG.12(a) with FIG.12(b), we found that when the defect layer is located in the middle of GFPCs, the electric field was weaken. While in FIG.12(c), the electric field was enhance. They are shown that both the defect layer and its' position have the effects on the distribution of light field, and we can find the defect layer made the electric field local enhanced for the conventional PCs. While the defect layer made the electric field whole enhanced or decreased for the GFPCs.

In FIG.13, we shall consider the effect of half period number N $((BA)^N D(BA)^N)$ on the electric field. Taken $N = 4$, $N = 6$ and $N = 8$ corresponding to FIG.13(a-c). The results shown that when N increase, the relative intensity of electric field heighten.

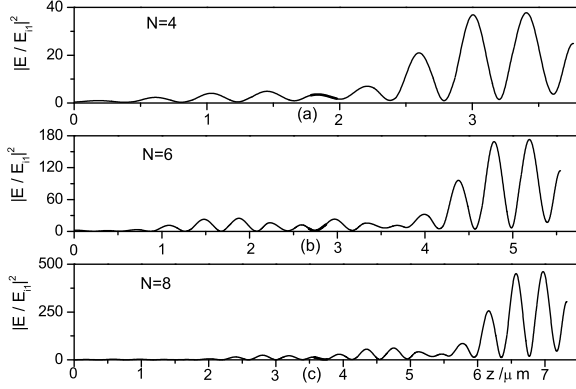


FIG. 13: The light field distribution of the GFPCs $((BA)^N D(BA)^N)$ with different periodicity, (a) $N=4$, (b) $N=6$, (c) $N=8$. The bold line is the field distribution of defect layer.

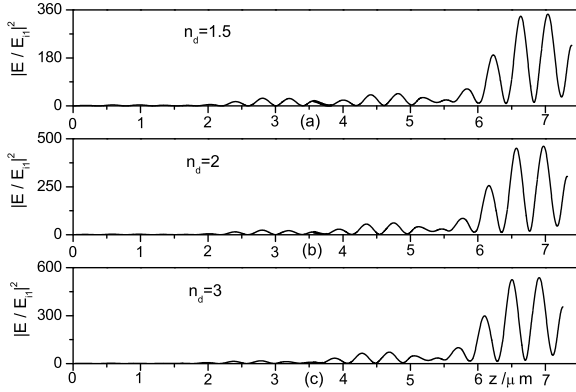


FIG. 14: The light field distribution of the GFPCs $((BA)^8 D(BA)^8)$ with different refractive indexes of defect layer. The bold line is the field distribution of defect layer.

FIG.14 show the effect of different refractive indexes of defect layer (n_d) on the electric field. The structure is $(BA)^8 D(BA)^8$. In FIG.14(a-c), n_d are equal to 1.5, 2 and 3, respectively. As we can see in FIG.14(a-c), when n_d increase, the relative intensity of electric field was enhanced.

6. Conclusion

In summary, We have theoretically investigated a new general function photonic crystals (GFPCs) with defect layer. Based on Fermat principle, we achieve the motion equations of light in one-dimensional general function photonic crystals, and calculate its transfer matrix. We choose the line refractive index function for two mediums A and B , and obtain some results: (1) When the position of defect layer move behind in the GFPCs, or the refractive indexes of defect layer increase, the transmission intensity maximum of defect model decreases. (2) When the period number of GFPCs increase, the transmission intensity of defect model increase, and the defect model's width of half height become narrow. (3) Both the defect layer and it's position have the effects on the electric field. (4) In the structure $(BA)^N D(BA)^N$, when the period number N increase, the relative intensity of electric field increase. (5) When the refractive indexes of defect layer (n_d) increase, the relative intensity of electric field was enhanced. Since the GFPCs has new character different from the conventional PCs, it should be helpful in the design of photonic crystals.

-
- [1] E. Yablonovitch, Phys. Rev. Lett. **58**, 2059C2062 (1987).
 - [2] J. D. Joannopoulos, P. R. Villeneuve, and S. Fan, Nature **386**, 143-149 (1997).
 - [3] P. Russell, Photonic crystal fibers, Science **299**, 358-362 (2003).
 - [4] J. C. Knight, Photonic crystal fibres, Nature **424**, 847-851 (2003).
 - [5] A. F. Abouraddy, M. Bayindir, G. Benoit, S. D. Hart, K. Kuriki, N. Orf, O. Shapira, F. Sorin, B. Temelkuranl, and Y. Fink, Nature Photonics **6**, 336-347 (2007).
 - [6] S. John, Phys. Rev. Lett. **58**, 2486-2489 (1987).
 - [7] P. Nedel, X. Letartre, C. Seassal, A. Auffves, L. Ferrier, E. Drouard, A. Rahmani, and P. Viktorovitch., Optics Express. **19** 5014 (2011).
 - [8] C. Zinoni, B. Alloing, L. H. Li, F. Marsili, A. Fiore, L. Lunghi, A. Gerardino, Yu. B. Vakhtomin, K. V. Smirnov, and G. N. Gol'tsman., Appl. Phys. Lett. **91** 031106 (2007).
 - [9] S. G. Johnson and J. D. Joannopoulos., Optics Express. **8** 173 (2001).
 - [10] V. S. C. Manga Rao and S. Hughes., Phys. Rev. Lett. **99** 193901 (2007).
 - [11] G. Lecamp, P. Lalanne, and J. P. Hugonin., Phys. Rev. Lett. **99** 023902 (2007).
 - [12] V. S. C. Manga Rao and S. Hughes., Phys. Rev B **75** 205437 (2007).
 - [13] T. Lund-Hansen, S. Stobbe, B. Julsgaard, H. Thyrrstrup, T. Snner, M. Kamp, A. Forchel, and P. Lodahl., Phys. Rev. Lett. **101** 113903 (2008).
 - [14] S. J. Dewhurst, D. Granados, D. J. P. Ellis, A. J. Bennett, R. B. Patel, I. Farrer, D. Anderson, G. A. C. Jones, D. A. Ritchie, and A. J. Shields., Appl. Phys. Lett. **96** 031109

- (2010).
- [15] K. Busch and S. John, Phys. Rev. Lett. **83**, 967 (1999).
 - [16] J-K. Yang, H. Noh, M. J. Rooks, G. S. Solomon, F. Vollmer and H. Cao., Appl. Phys. Lett. 98, 241107 (2011)
 - [17] R. Martinez-Sala, J. Sancho, J. V. Sanchez, V. Gomez, J. Llinares and F. Meseguer, nature **378**, 241 (1995).
 - [18] D. Torrent, A. Hakansson, F. Cervera and J. Sanchez - Dehesa, Phys. Rev. Lett. **96**, 204302 (2006).
 - [19] J. D. Joannopoulos, R. D. Meade, and J. N. Winn, Photonic Crystals, Princeton University Press, Princeton (1995).
 - [20] G. Guida, A. Lustrac and A. Priou, An introduction to Photonic Band Gap (PBG) materials, Progress In Electromagnetics Research, PIER, Vol. 41, 1C20 (2003).
 - [21] K. Bush, S. Lolkes, R. B. Wehrspohn and H. Foll, Photonic Crystals, Wiley, Berlin (2006).
 - [22] Xiang-Yao Wu Bai-Jun Zhang Jing-Hai Yang, Xiao-Jing Liu Nuo Ba Yi-Heng Wu and Qing-Cai Wang Physica E **43**, 1694-1700 (2011).
 - [23] Xiang-Yao Wu Bo-Jun Zhang Xiao-Jing Liu Nuo Ba Si-Qi Zhang Jing Wang Physica E **44**, 1223-1229 (2012).
 - [24] Xiang-Yao Wu Bo-Jun Zhang Jing-Hai Yang Si-Qi Zhang Xiao-Jing Liu Jing Wang, Nuo Ba, Zhong Hua and Xin-Guo Yin, Physica E **45**, 166-172 (2012).
 - [25] Xiang-Yao Wu Bo-Jun Zhang Xiao-Jing Liu Si-Qi Zhang Jing Wang, Nuo Ba, Li Xiao and Hong Li Physica E **46**, 133-138 (2012).